

Unified equivalent frame method for post-tensioned flat plate slab structures

Seung-Ho Choi^{1a}, Deuck Hang Lee^{2b}, Jae-Yuel Oh^{1c}, Kang Su Kim^{*1}, Jae-Yeon Lee^{3d}
and Kang Seok Lee^{4e}

¹Department of Architectural Engineering, University of Seoul, 163 Siripdaero, Dongdaemun-gu, Seoul, 02504, Korea

²Department of Civil Engineering, Nazarbayev University, Kabanbay Batyr Ave 53, Astana 010000, Kazakhstan

³Division of Architecture, Mokwon University, 88 Doanbuk-ro, Seo-gu, Daejeon, 35349, Korea

⁴School of Architecture, Chonnam National University, 77 Yongbong-ro, Buk-gu, Gwangju, 61186, Korea

(Received July 21, 2017, Revised August 28, 2017, Accepted September 2, 2017)

Abstract. The post-tensioned (PT) flat plate slab system is commonly used in practice, and this simple and fast construction method is also considered to be a very efficient method because it can provide excellent deflection and crack control performance under a service load condition and consequently can be advantageous when applying to long-span structures. However, a detailed design guideline for evaluating the lateral behavior of the PT flat plate slab system is not available in current design codes. Thus, typical design methods used for conventional reinforced concrete (RC) flat plate slab structures have inevitably been adopted in practice for the lateral load design of PT flat plate structures. In the authors' previous studies, the unified equivalent frame method (UEFM) was proposed, which considers the combined effect of gravity and lateral loads for the lateral behavior analysis of RC flat plate slab structures. The aim of this study is to extend the concept of the UEFM to the lateral analysis of PT flat plate slab structures. In addition, the stiffness reduction factors of torsional members on interior and exterior equivalent frames were newly introduced considering the effect of post-tensioning. Test results of various PT flat plate slab-column connection specimens were collected from literature, and compared to the analysis results estimated by the extended UEFM.

Keywords: post-tension; flat plate; slab; lateral load; gravity load; equivalent frame; stiffness reduction

1. Introduction

The flat plate slab system has been commonly used in building constructions, including offices, residential, and parking structures, as a gravity force resisting system (GFRS). In the flat plate system, slabs are directly supported on column members without beams, which leads to a reduction in story heights. Also, superior constructability can also be achieved due to its simple formwork compared to a typical reinforced concrete (RC) beam-column system (Hwang and Moehle 1993, 2000, Kim and Lee 2005, Park *et al.* 2012, Görkem and Hüsem 2013, Kang *et al.* 2013, Mirzaei and Sasani 2013, Kim *et al.* 2014, Kim *et al.* 2014, Kotsoviu *et al.* 2016, Kurtoğlu *et al.* 2016, Kim and Kang 2017, Hegger *et al.* 2017). The current

design codes (ACI 318-14, BS 8110, Eurocode 2, and KCI-M-12) permit the equivalent frame method (EFM) to be used for design or analysis of the flat plate structures subjected to gravity and lateral loads. In the EFM, a 3D slab-column frame system is equivalently converted to a series of 2D planar frames for a simple analysis. However, the EFM presented in the design codes was initially developed for the analysis of the RC flat plate frame system subjected to gravity loads only, which implies that this method is not in fact suitable for the analysis of the flat plate structure subjected to lateral loads or combined gravity and lateral loads. This is because the load transfer mechanism of the flat plate system subjected to lateral loads is quite different from that subjected to gravity loads only (Hwang and Moehle 2000, Park *et al.* 2009, Kim *et al.* 2014). To overcome such a limitation of the EFM, Kim *et al.* (2014) and Choi *et al.* (2014) proposed a torsional stiffness evaluation model that can consider the combined effects of gravity and lateral loads for the RC flat plate slab system, and the nonlinear lateral analysis method suitable for the RC flat plate slab structure subjected to combined gravity and lateral loads was named as the unified equivalent frame method (UEFM).

By utilizing prestressing forces, the PT flat plate slab system has an excellent deflection control performance at service loads as well as high flexural and shear capacities at ultimate (Lee *et al.* 2014, Hwang *et al.* 2015, Mohammed and Taysi 2017), and thus this system is more suitable for long span structures than the RC flat plate slab system. In addition, due to the increasing demand for long-span slab

*Corresponding author, Professor

E-mail: kangkim@uos.ac.kr

^aPh.D. Candidate

E-mail: ssarmilmil@hanmail.net

^bAssistant Professor

E-mail: deuckhang.lee@nu.edu.kz

^cPh.D. Candidate

E-mail: hahappyppy@naver.com

^dProfessor

E-mail: jylee@mu.ac.kr

^eProfessor

E-mail: kslnist@jnu.ac.kr

systems in construction market, researchers have conducted many studies on the lateral behavior of the flat plate slab system (Kang 2004, Ritchie and Ghali 2005, Gayed and Ghali 2006, Han *et al.* 2006, Karimiyan *et al.* 2014). Since no proper analysis method or detailed design guideline is available for the PT flat plate slab system, the EFM, developed for the conventional RC flat plate slab system, has been inevitably adopted in practice for the gravity and lateral load design of the PT flat plate slab system. In addition, the stiffness reduction of the PT flat plate slab system when subjected to lateral loads is a very important issue that needs to be investigated in detail. The aim of this study is to extend the main formula and concept of the UEFM to the lateral behavioral analysis of the PT flat plate slab system. In particular, the stiffness reduction factors of the torsional members of exterior and interior equivalent frames were newly introduced to consider the effect of the post-tensioning, and the proposed method were also examined by comparing the analysis results to the test results of the PT flat plate slab specimens.

2. Review of previous studies

2.1 Equivalent frame method (EFM) and modified equivalent frame method (MEFM)

In order to equivalently convert a 3D slab-column frame to a 2D planar frame, the stiffness of an equivalent column in the EFM is determined by summing up the flexibilities of columns and torsional member. The stiffness of an equivalent column (K_{ec}) can be expressed, as follows

$$\frac{1}{K_{ec}} = \frac{1}{\sum K_c} + \frac{1}{K_{tg}} \quad (1)$$

where K_c and K_{tg} are the flexural stiffness of the column and the torsional stiffness of the torsional member in the RC flat plate slab system under gravity loads, respectively. The ACI 318-14 (2014) and KCI-M-12 (2012) present the torsional stiffness (K_{tg}), as follows

$$K_{tg} = \frac{9CE_c}{L_2 \left(1 - \frac{c_2}{L_2}\right)^3} \quad (2)$$

where C is the torsional constant, E_c is the elastic modulus of concrete, and L_2 and c_2 are the span length and the column width perpendicular to the design direction, respectively.

Park *et al.* (2009) proposed a modified equivalent frame method (MEFM) to evaluate the lateral stiffness of the flat plate slab system subjected to lateral loads. When lateral loads are dominant, the column member is deformed first by the lateral loads, and the flexural moments are then transferred to the slab member through the torsional member. Thus, the MEFM adopted the concept of the equivalent slab (Vanderbilt 1979, 1981, Vanderbilt and Corley 1983). The rotational angle of the equivalent slab can be estimated by summing the rotational angle of the

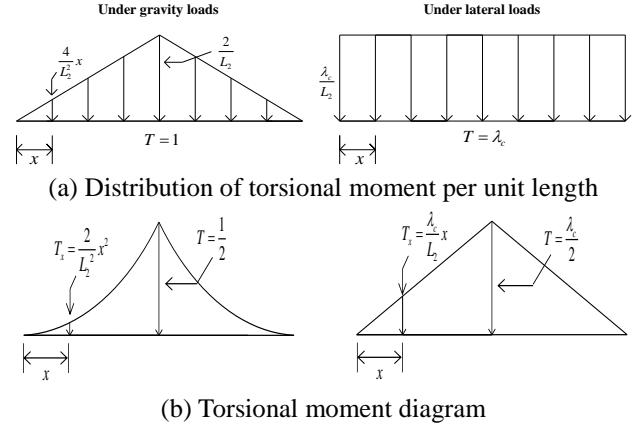


Fig. 1 Concept of load ratio factor (UEFM) (Kim *et al.* 2014)

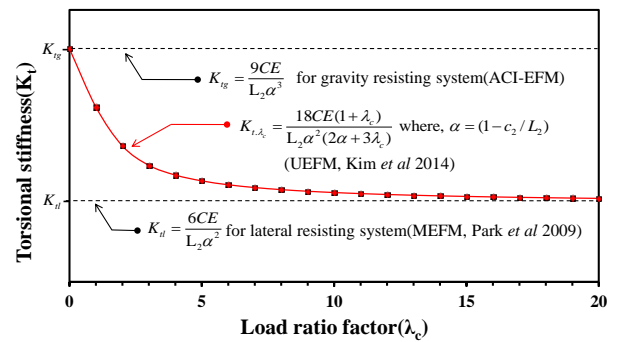


Fig. 2 Determination of torsional stiffness using load ratio factor (Kim *et al.* 2014)

slab and the average rotational angle of the torsional member. Thus, the stiffness of the equivalent slab (K_{es}) can be expressed, as follows

$$\frac{1}{K_{es}} = \frac{1}{\sum K_s} + \frac{1}{K_{tl}} \quad (3)$$

where K_s is the flexural stiffness of the slab and K_{tl} is the torsional stiffness of the torsional member in the flat system under lateral loads. In the MEFM (Park *et al.* 2009), the torsional stiffness (K_{tl}) was presented, as follows

$$K_{tl} = \frac{6CE_c}{L_2 \left(1 - \frac{c_2}{L_2}\right)^2} \quad (4)$$

2.2 Unified equivalent frame method (UEFM)

According to the EFM, if the unit torsional moment induced by gravity loads is applied to the equivalent column, the torsional moment is distributed in a triangular shape. This is because the stiffness of the column member is larger than that of the slab member, and the effect of the column stiffness on the moment distribution is reduced as the distance from the column increases (Corely and Jirsa 1970). In contrast, according to Park *et al.* (2009), when the unit torsional moment induced by lateral loads is applied to

the equivalent slab, the torsional moment is uniformly distributed on the torsional member. However, in a real situation, both gravity and lateral loads act simultaneously, and thus the moment distribution is affected by the combination of the gravity and lateral loads. To reflect this combined effect, as shown in Fig. 1, Kim *et al.* (2014) introduced the load ratio factor (λ_c), which can be defined as the relative ratio of the torsional moment induced by lateral loads (T_l) to that induced by gravity loads (T_g), as follows

$$\lambda_c = \frac{T_l}{T_g} \quad (5)$$

According to Kim *et al.* (2014), the effective stiffness of a torsional member in the flat plate slab system subjected to gravity and lateral loads (K_t, λ_c) can be also derived, as follows

$$K_{t,\lambda_c} = \frac{T_{tot}}{\theta_{tot}} = \frac{18CE(1+\lambda_c)}{L_2\alpha^2(2\alpha+3\lambda_c)} \quad (6)$$

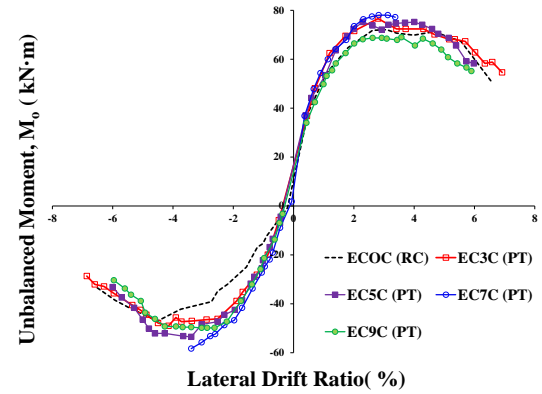
where T_{tot} is the total moment in the torsional member due to gravity and lateral loads, θ_{tot} is the rotation angle of the torsional member in the flat plate system subjected to gravity and lateral loads, and α is taken to be $1-c_2/L_2$. As shown in Fig. 2, the torsional stiffness obtained from the Eq. (6) is identical to that of the EFM for the case governed by gravity loads (i.e., $\lambda_c=0$). On the other hand, when the effect of lateral loads is very significant compared to that of gravity loads (i.e., $\lambda_c=\infty$), the torsional stiffness converges to that of the MEFM. It is worthy of emphasizing that the UEFM can rationally reflect the combined effect of lateral and gravity loads including the two extreme load cases, i.e., gravity loads only and lateral loads only. In this study, it is assumed that some portion of the total rotational angle developed in the torsional member ($\theta_{t,gravity}$) contributes to the rotation of the equivalent column, and the remaining portion of the rotation angle of the torsional member ($\theta_{t,lateral}$) can be considered as contributing to the rotation of the equivalent slab. On this basis, the flexibility of the equivalent column and the equivalent slab can be then expressed, respectively, as follows

$$\frac{1}{K_{ec}} = \frac{\sum K_c}{\sum K_c + \sum K_s} \frac{1}{K_{t,\lambda_c}} + \frac{1}{\sum K_c} \quad (7)$$

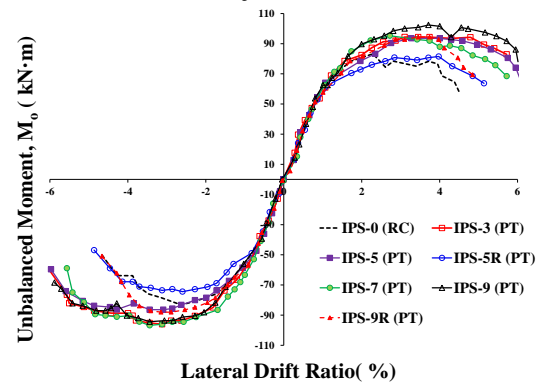
$$\frac{1}{K_{es}} = \frac{\sum K_s}{\sum K_c + \sum K_s} \frac{1}{K_{t,\lambda_c}} + \frac{1}{\sum K_s} \quad (8)$$

3. Unified equivalent frame method for PT flat plate considering stiffness reduction

Ritchie and Ghali (2005) and Gayed and Ghali (2006) conducted cyclic loading tests on post-tensioned exterior and interior slab-column connections, respectively. In their test programs, the key test variables were the relative reinforcement ratios between the prestressed steel (A_p) to



(a) Exterior slab-column joints (Ritchie and Ghali 2005)



(b) Interior slab-column joints (Gayed and Ghali 2006)

Fig. 3 Envelopes of unbalanced moment-drift ratio hysteresis loops

nonprestressed steel (A_s) and the magnitudes of the prestressing forces, while the flexural strengths of all the test specimens were set to be identical. As shown in Fig. 3, their test results showed that there was no significant difference in the lateral responses within the elastic range between the RC and PT slab-column connections, while the prestressed specimens showed greater energy dissipation capacity with delayed stiffness reduction compared to the nonprestressed specimens. This suggests that the UEFM can be extended to PT flat plate slabs as well as RC flat plate slabs within the elastic range. In concrete structures, cracks are inevitably induced by gravity and lateral loads. Thus, as the lateral load increases, the flexural stiffness of flat plate structures is reduced by the cracking and inelastic behavior of materials as well. Since the UEFM was developed for the elastic analysis of the flat plate systems, it is not suitable to analyze their nonlinear behavior after cracking, where the stiffness reduction is significant. While the nonlinear behavior of the flat plate slab systems can be captured well by finite element methods, they typically require considerable amounts of computational efforts, and the reliability of the analysis results largely depends on the expertise of the user (Cano and Klingner 1988, Ghobarah 2001, Park *et al.* 2009). Thus, many studies (Qaisrani 1993, Park *et al.* 2012) proposed simple analysis methods to consider the nonlinear lateral behavior of the post-tension flat plate system.

In the previous studies, the slab stiffness was reduced by a function of external loads only based on the effective

beam width model, and thus these approaches cannot be adopted in the UEFM due to the conceptual differences. Furthermore, the stiffness reduction in a structural system is largely affected not only by the stiffness reduction of the slabs, but also by the stiffness reduction of the columns and connections. Therefore, a new stiffness reduction model for the UEFM is required to properly consider the stiffness degradation mechanisms of PT flat plate systems. Choi *et al.* (2014) proposed a method that could simply reflect the stiffness reductions of the slab-column connections, the equivalent columns, and the equivalent slabs by reducing the stiffness of the torsional members. In this study, the stiffness degradation in the structural system is considered by reducing the stiffness of the torsional member as proposed by Choi *et al.* (2014), and the effect of the compressive stress introduced in the slab is also considered.

3.1 Stiffness reduction due to gravity shear

The actual flexural stiffness of the flat plate slab (K_I) is generally smaller than the elastic flexural stiffness (K_0) calculated using the gross section of the slab without a consideration of gravity loads (Schwaighofer and Collins, 1977, Hwang and Moehle 2000, Choi and Park 2003).

Choi and Park (2003) thus proposed the stiffness reduction factor of the slab (η_g) as a function of the gravity-shear ratio (V_g/V_c) based on their numerical analysis results, as follows

$$\eta_g = \frac{K_I}{K_0} = \frac{1}{1.7(V_g/V_c) + 1} \quad (9)$$

where V_c is the punching shear strength of the flat plate slab, which can be estimated, as follows

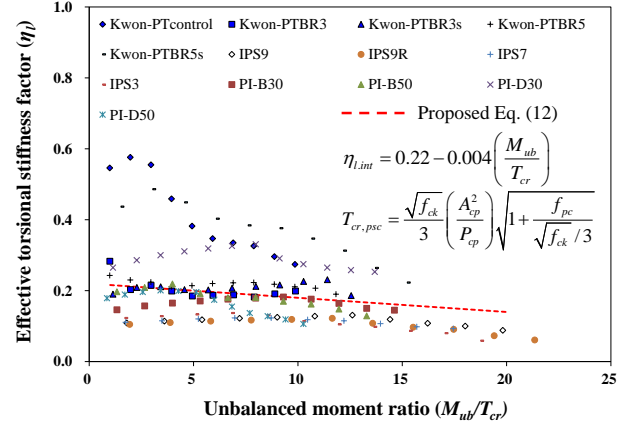
$$V_c = \phi(\beta_p \sqrt{f_{ck}} + 0.3f_{pc})b_o d + V_p \quad (10)$$

where β_p is adopted as the smaller of 0.29 and $(a_s d/b_o + 1.5)/12$. In addition, a_s is taken to be 40 for interior columns, 30 for exterior columns, and 20 for corner columns, while V_p is the vertical component of effective prestressing forces. In this study, the effective flexural stiffness of the slab-beam member ($K_{s,eff}$) is used as the slab stiffness (K_s) with a consideration of the initial slab stiffness degradation due to the gravity shear (V_g), as follows

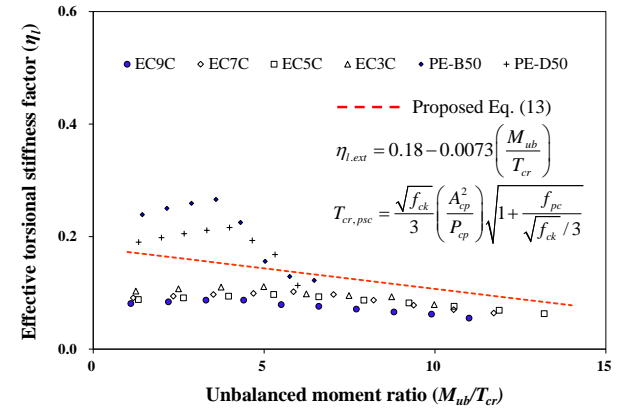
$$K_{s,eff} = \eta_g K_s \quad (11)$$

3.2 Stiffness reduction due to unbalanced moment induced by gravity and lateral loads

Choi *et al.* (2014) proposed the stiffness reduction factor for the torsional member (η_t) as a function of the unbalanced moment (M_{ub}) and the cracking strength of the torsional member (T_{cr}) based on the collected test results. They collected 16 interior slab-column connection specimens and 9 exterior slab-column connection specimens to determine the stiffness reduction factors of the torsional members, and significant relations were found between the unbalanced moment (M_{ub}) and the stiffness degradation behaviors of the flat plate systems. Choi *et al.*



(a) Interior slab-column joints



(b) Exterior slab-column joints

Fig. 4 Stiffness degradation of torsional members with respect to unbalanced moment ratio

(2014) then presented the stiffness reduction factors of the torsional members for the interior and exterior connections ($\eta_{t,int}$ and $\eta_{t,ext}$), respectively, as follows

$$\eta_{t,int} = 0.22 - 0.004 \left(\frac{M_{ub}}{T_{cr}} \right) \quad (12)$$

$$\eta_{t,ext} = 0.18 - 0.0073 \left(\frac{M_{ub}}{T_{cr}} \right) \quad (13)$$

where, the cracking strength of the torsional member (T_{cr}) is taken as $1/3 \sqrt{f'_c} A_{cp}^2 / p_{cp}$ based on the ACI 318-14 (2014). Here, f'_c is the compressive strength of concrete, A_{cp} is the sectional area of the shear flow zone, i.e., $c_1 t$, where c_1 is the column width in the loading direction, and t is the slab thickness. Also, p_{cp} is the perimeter of the shear flow zone, i.e., $2(c_1 + t)$.

For the extension of the stiffness reduction factor model, which was proposed for the RC flat plate by Choi *et al.* (2014), to the PT flat plate structure, the effect of the prestress (f_{pc}) shall be considered in the cracking strength of the torsional member in PT flat plate structures ($T_{cr,pse}$). The principal tensile stress (f_t) developed in the torsional member can be estimated from the Mohr's stress circle, as follows

Table 1 Dimensions, material properties, and gravity loads of Post-tensioned slab-column connection specimens

Researchers Label	Joint type ^c	Dimensions (mm)						Gravity load			f'_c (MPa)	f_{pc} (MPa)	
		L_1	L_2	t	c_1	c_2	H	d_{ave}	V_g (kN)	V_g/V_c			
Kwon <i>et al.</i> (2007)	PT-BR3	Int	4000	3600	110	300	300	1800	92.4	203.8	0.46	29.85	1.68
	PT-BR3s	Int	4000	3600	110	300	300	1800	92.4	184.6	0.46	30.09	1.15
	PT-BR5	Int	4000	3600	110	300	300	1800	92.4	206.8	0.46	30.17	1.68
	PT-BR5s	Int	4000	3600	110	300	300	1800	92.4	185.5	0.46	29.95	1.15
Kee <i>et al.</i> (2006)	PI-B30	Int	4800	3600	132	300	300	2100	104.2	81.0	0.24	32.3	1.21
	PI-B50	Int	4800	3600	132	300	300	2100	104.2	132.2	0.39	32.3	1.21
	PI-D30	Int	4800	3600	132	300	300	2100	104.2	81.0	0.24	32.3	1.21
	PI-D50	Int	4800	3600	132	300	300	2100	104.2	132.2	0.39	32.3	1.21
Gayed and Ghali (2006)	IPS-3	Int	1900	1900	150	250	250	1400	114	240	0.84	27	0.40
	IPS-7	Int	1900	1900	150	250	250	1400	114	240	0.74	31	0.90
	IPS-9	Int	1900	1900	150	250	250	1400	114	240	0.79	23	1.10
	IPS-9R	Int	1900	1900	150	250	250	1400	114	240	0.76	26	1.10
Han <i>et al.</i> (2006)	PE-B50	Ext	2400	3600	130	300	300	2100	110	84.2	0.34	32.3	1.21
	PE-D50	Ext	2400	3600	130	300	300	2100	110	80.2	0.32	32.3	1.21
Ritchie and Ghali (2005)	EC3C	Ext	1350	1900	150	250	250	1400	114	110	0.67	25.8	0.40
	EC5C	Ext	1350	1900	150	250	250	1400	114	110	0.64	25.6	0.66
	EC7C	Ext	1350	1900	150	250	250	1400	114	110	0.60	29.4	0.85
	EC9C	Ext	1350	1900	150	250	250	1400	114	110	0.57	28.2	1.10

^aInt: internal; Ext: external

Notation: L_1 : span length width the design direction, L_2 : span length width perpendicular to the design direction, t : slab thickness, c_1 : column width in the loading direction, c_2 : column width perpendicular to the design direction, H : height of column, d_{ave} : average effective depth of slab, V_g : gravity shear force, V_g/V_c : gravity shear ratio, f'_c : compressive strength of concrete, f_{pc} : compressive stress due to the prestress

$$f_1 = \sqrt{v^2 + \left(\frac{f_{pc}}{2}\right)^2} - \frac{f_{pc}}{2} \quad (14)$$

where, v is the shear stress on the web. When the principal tensile stress (f_1) reaches the cracking strength of concrete (f_{cr}), it is assumed that diagonal cracking occurs, at which the shear stress (v) can be defined as the shear cracking strength (v_{cr}), as follows

$$v_{cr} = f_{cr} \sqrt{1 + \frac{f_{pc}}{f_{cr}}} \quad (15)$$

Therefore, the cracking strength of the torsional member considering the prestress effect ($T_{cr,psc}$) can be estimated, as follows (ACI 318-14)

$$T_{cr,psc} = \frac{\sqrt{f_{ck}}}{3} \left(\frac{A_{cp}^2}{P_{cp}} \right) \sqrt{1 + \frac{f_{pc}}{\sqrt{f_{ck}}/3}} \quad (16)$$

In Eqs. (12) and (13), the stiffness reduction factors of the torsional members in the PT interior and exterior connections ($\eta_{l,int}$ and $\eta_{l,ext}$) are greater than those in the RC connections due to increase of crack strength of the torsional members by considering the prestress effect ($T_{cr,psc}$). This approach can rationally reflect the improved stiffness of the PT flat plate slab system compared to that of

the RC flat plate slab system. Fig. 4 shows the comparisons of the stiffness reduction factors of the torsional members for the interior and exterior PT connections ($\eta_{l,int}$ and $\eta_{l,ext}$) considering the prestress effect in the cracking moment ($T_{cr,psc}$) and those estimated from the test results. The stiffness reduction factors calculated using Eqs. (12), (13) and (16) closely evaluated the stiffness degradation trend for the PT connection specimens as the unbalanced moment ratio increases.

The flexibility of the equivalent slab and the equivalent column ($1/K_{es}$ and $1/K_{ec}$) considering the stiffness reduction factors due to gravity loads and lateral loads can be estimated, respectively, as follows

$$\frac{1}{K_{es}} = \theta_{t,lateral} + \theta_c = \frac{\sum K_{s,eff}}{\sum K_c + \sum K_{s,eff}} \frac{1}{\eta_l K_{t,\lambda_c}} + \frac{1}{\sum K_{s,eff}} \quad (17)$$

$$\frac{1}{K_{ec}} = \theta_{t,gravity} + \theta_c = \frac{\sum K_c}{\sum K_c + \sum K_{s,eff}} \frac{1}{\eta_l K_{t,\lambda_c}} + \frac{1}{\sum K_c} \quad (18)$$

where $\theta_{t,gravity}$ and $\theta_{t,lateral}$ are the rotation angle of the torsional member in the PT flat plate slab system subjected to gravity and lateral loads, respectively, and θ_c is the rotation angle of the column.

4. Validation of the unified equivalent frame method

As shown in Table 1, a total of 18 interior and exterior PT flat plate slab-column connection specimens were collected from previous studies to verify the accuracy of the UEFM proposed in this study. Kwon *et al.* (2007) conducted lateral cyclic tests on the interior PT connections with a gravity shear ratio (V_g/V_c) of 0.46, where the key test variables were the magnitude of the prestress (f_{pc}) and the effect of bonded reinforcement. Kee *et al.* (2006) also conducted tests on the interior PT slab-column connection specimens with f_{pc} of 1.21 MPa, and the effects of the gravity shear forces (V_g/V_c) and the tendon layout were also investigated.

The interior PT slab-column connection specimens with high gravity shear ratios ranging from 0.76 to 0.81 were tested by Gayed and Ghali (2006). Han *et al.* (2006) also conducted cyclic tests on the PT flat plate connections with a moderate level of gravity shear ratios (V_g/V_c) between 0.32 and 0.34, in which the concentrated and uniformly-distributed tendon layout was considered. Ritchie and Ghali (2005) tested the exterior PT flat plate slab-column connections with relatively high gravity shear ratios (V_g/V_c) ranging from 0.57 to 0.67, whereby the level of prestress (f_{pc}) was the key test variable.

Figs. 5 and 6 show the comparisons between the lateral responses of the PT interior and exterior connections collected from literatures (Kwon *et al.* 2007, Kee *et al.* 2006, Gayed and Ghali 2006, Han *et al.* 2006, Ritchie and Ghali 2005) and those estimated from the UEFM with the stiffness reduction factors, where the analysis results were represented by red round markers. The lateral analysis was terminated at the maximum allowable drift ratio (DR_{max}), expressed as follows (ACI 318-14)

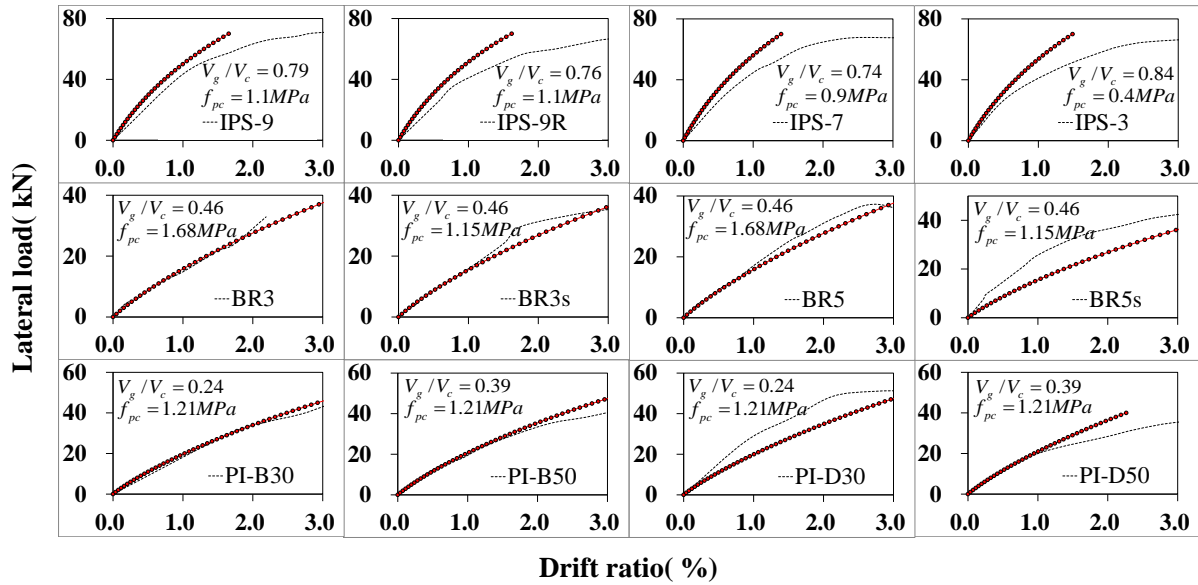


Fig. 5 Evaluation of the proposed model (Interior slab-column connections)

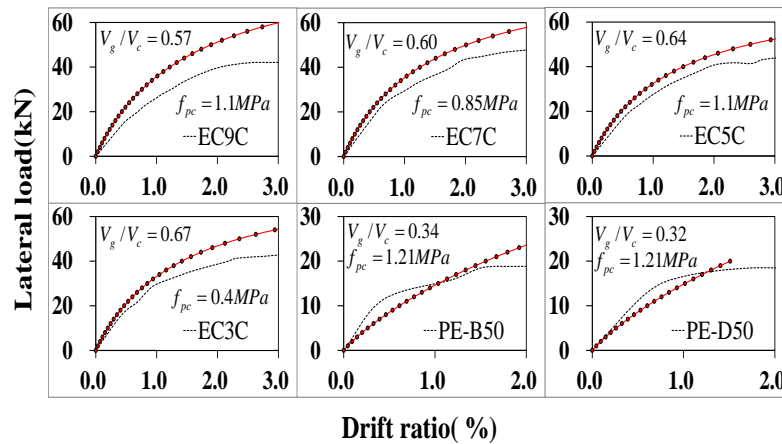


Fig. 6 Evaluation of the proposed model (Exterior slab-column connections)

$$DR_{\max} = 0.035 - 0.05(V_g / \phi V_c) \quad (19)$$

where ϕ is the strength reduction factor, V_c is the punching shear strength of the reinforced concrete flat plate slab. Eq. (19) is actually the maximum allowable drift ratio of reinforced concrete flat plate system without shear reinforcement specified in ACI 318. In this study, it was applied to the post-tensioned flat plate system without shear reinforcement by replacing V_c to the punching shear strength of the post-tensioned flat plate system without shear reinforcement expressed in Eq. (10), and the strength reduction factor ϕ was set to 1.0 for the analysis purpose.

The proposed model provides good estimations on the lateral behavior of the test specimens, including not only the test results by Gayed and Ghali (2006), whose gravity shear ratios were relatively high up to 0.7, but also the interior and exterior slab-column connection specimens with a low level of gravity-shear ratios. It is thus considered that the proposed model can properly reflect the influence of the gravity shear ratios (V_g/V_c) and the magnitudes of the prestress (f_{pc}).

5. Conclusions

This study briefly introduced the main formulations of the UEFM proposed in the authors' previous study, and the concept of the UEFM was extended to the PT flat plate slab systems. The stiffness reduction factors of the torsional members that can easily consider the stiffness reduction behavior of PT flat plate systems were also presented. From this study, the following conclusions can be drawn:

1. This study proposed a lateral behavior analysis method for PT flat plate slab systems subjected to combined gravity and lateral loads. It appeared that the UEFM can be properly extended to the PT flat plate slab systems.
2. This study proposed the stiffness reduction factors of the torsional members in the PT flat plate slab system. The proposed stiffness reduction factors successfully captured the stiffness degradation behaviors of the PT flat plate slab structures considering the improved cracking strength of the torsional members due to post-tensioning.
3. The proposed UEFM accurately evaluated the lateral behaviors of the interior and exterior PT connection specimens with various levels of the gravity shear ratios

(V_g/V_c) and prestress (f_{pc}).

Acknowledgments

This research was supported by the National Research Foundation of Korea (NRF) (2017R1D1A3B03028005).

References

- ACI Committee 318 (2014), *Building Code Requirements for Structural Concrete and Commentary* (ACI 318-14), American Concrete Institute, Farmington Hills, Michigan, U.S.A.
- Cano, M.T. and Kilgner, R.E. (1988), "Comparison of analysis procedures for two-way slabs", *ACI Struct. J.*, **85**(6), 597-608.
- Choi, K.K. and Park, H.G. (2003), "Moment-rotation relationship and effective stiffness of flat plates under lateral load", *J. Kor. Concrete Inst.*, **15**(6), 856-865.
- Choi, S.H., Lee, D.H., Oh, J.Y., Kim, K.S., Lee, J.Y. and Shin, M.S. (2014), "Unified equivalent frame method for flat plate slab structures under combined gravity and lateral loads-part 2: Verification", *Earthq. Struct.*, **7**(5), 735-751.
- Corley, W.G. and Jirsa, J.O. (1970), "Equivalent frame analysis for slab design", *ACI J. Proc.*, **67**(11), 875-884.
- Gayed, R.B. and Ghali, A. (2006), "Seismic-resistant joints of interior columns with prestressed slabs", *ACI Struct. J.*, **103**(5), 710-719.
- Ghobarah, A. (2001), "Performance-based design in earthquake engineering: State of development", *Eng. Struct.*, **23**(8), 878-884.
- Görkem, S.E. and Hüsem, M. (2013), "Load capacity of high-strength reinforced concrete slabs by yield line theory", *Comput. Concrete*, **12**(6), 819-829.
- Han, S.W., Kee, S.H., Park, Y.M., Lee, L.H. and Kang, T.H.K. (2006), "Hysteretic behavior of exterior post-tensioned flat plate connections", *Eng. Struct.*, **28**(14), 1983-1996.
- Hegger, J., Sherif, A.G., Kueres, D. and Siburg, C. (2017), "Efficiency of various punching shear reinforcement systems for flat slabs", *ACI Struct. J.*, **114**(3), 631-642.
- Hwang, J.H., Lee, D.H., Park, M.K., Choi, S.H., Kim, K.S. and Pan, Z. (2015), "Shear performance assessment of steel fiber reinforced-prestressed concrete members", *Comput. Concrete*, **16**(6), 825-846.
- Hwang, S.J. and Moehle, J.P. (1993), *An Experimental Study of Flat-Plate Structures under Vertical and Lateral Loads*, Report No. UCB/EERC-93/03, University of California, Berkeley, California, U.S.A.
- Hwang, S.J. and Moehle, J.P. (2000), "Models for laterally loaded slab-column frames", *ACI Struct. J.*, **97**(2), 345-352.
- Kang, S.M., Eom, T.S. and Kim, J.Y. (2013), "Reshoring effects on deflection of multi-shored flat plate systems under construction", *Struct. Eng. Mech.*, **45**(4), 455-470.
- Kang, T.H.K. (2004), "Shake table tests and analytical studies of reinforced and post-tensioned concrete flat plate frames", Ph.D. thesis, University of California, California, U.S.A.
- Karimiyan, S., Kashan, A.H. and Karimiyan, M. (2014), "Progressive collapse vulnerability in 6-story RC symmetric and asymmetric buildings under earthquake loads", *Earthq. Struct.*, **6**(5), 473-494.
- KCI-M-12 (2012), *Design Specifications for Concrete Structures*, Korea Concrete Institute, Korea.
- Kee, S.H., Han, S.W., Ha, S.S., Cho, K.H. and Lee, L.H. (2006), "Cyclic behavior of interior joints in post tensioned flat plate slab systems", *J. Archit. Inst. Kor.*, **22**(4), 39-46.
- Kim, H.S. and Lee, D.G. (2005), "Efficient analysis of flat slab structures subjected to lateral loads", *Eng. Struct.*, **27**(2), 251-263.
- Kim, J.Y. and Kang, S.M. (2017), "Simulations of short-and long-term deflections of flat plates considering effects of construction sequences", *Struct. Eng. Mech.*, **62**(4), 477-485.
- Kim, K.S., Choi, S.H., Ju, H.J., Lee, D.H., Lee, J.Y. and Shin, M.S. (2014), "Unified equivalent frame method for flat plate slab structures under combined gravity and lateral loads-part 1: Derivation", *Earthq. Struct.*, **7**(5), 719-733.
- Kim, U., Huang, Y., Chakrabarti, P.R. and Kang, T.H.K. (2014), "Modeling of post-tensioned one-way and two-way slabs with unbonded tendons", *Comput. Concrete*, **13**(5), 587-601.
- Kotsovou, G.M., Kotsovou, G.M. and Vougioukas, E. (2016), "Assessment of design methods for punching through numerical experiments", *Comput. Concrete*, **17**(3), 305-322.
- Kurtoglu, A.E., Çevik, A., Albegmrlı, H.M., Gülşan, M.E. and Bilgehan, M. (2016), "Reliability-based modeling of punching shear capacity of FRP-reinforced two-way slabs", *Comput. Concrete*, **17**(1), 87-106.
- Kwon, N.H., Lee, S.I. and Cho, Y.S. (2007), "Hysteretic behavior of interior column connections with post-tensioned flat plate slab designed for gravity system under lateral load", *J. Archit. Inst. Kor.*, **23**(7), 61-68.
- Lee, D.H., Park, M.K., Oh, J.Y., Kim, K.S., Im, J.H. and Seo, S.Y. (2014), "Web-shear capacity of prestressed hollow-core slab unit with consideration on the minimum shear reinforcement requirement", *Comput. Concrete*, **14**(3), 211-231.
- Mirzaei, Y. and Sasani, M. (2013), "Progressive collapse resistance of flat slabs: Modeling post-punching behavior", *Comput. Concrete*, **12**(3), 351-375.
- Mohammed, A.H. and Taysi, N. (2017), "Modeling of bonded and unbonded post-tensioned concrete flat slabs under flexural and thermal loading", *Struct. Eng. Mech.*, **62**(5), 595-606.
- Park, Y.M., Rew, Y.H. and Han, S.W. (2012), "Stiffness reduction factor for post-tensioned flat plate slabs", *Mag. Concrete Res.*, **64**(1), 83-92.
- Park, Y.M., Han, S.W. and Kee, S.H. (2009), "A modified equivalent frame method for lateral load analysis", *Mag. Concrete Res.*, **61**(5), 359-370.
- Qaisrani, A.N. (1993), "Interior post-tensioned flat-plate connections subjected to vertical and biaxial lateral loading", Ph.D. Dissertation, University of California, Berkeley, California, U.S.A.
- Ritchie, M. and Ghali, A. (2005), "Seismic-resistant connections of edge columns with prestressed slabs", *ACI Struct. J.*, **102**(2), 314-323.
- Schwaighofer, J. and Collins, M.P. (1977), "Experimental study of the behavior of reinforced concrete coupling slabs", *ACI J. Proc.*, **74**(3), 123-127.
- Vanderbilt, M.D. (1979), "Equivalent frame analysis for lateral loads. Proceedings", *ASCE J. Struct. Div.*, **105**(ST10), 1981-1998.
- Vanderbilt, M.D. (1981), *The Equivalent Frame Analysis for Reinforced Concrete Slabs*, Structural Research Series No. 36, Civil Engineering Department, Colorado State University, Fort Collins, U.S.A.
- Vanderbilt, M.D. and Corley, W.G. (1983), "Frame analysis for concrete buildings", *Concrete Int.*, **5**(12), 33-43.

Notations

		t	Slab thickness
A_{cp}	Sectional area of the shear flow zone	T_{cr}	Cracking strength of the torsional member
A_p	Prestressed steel	$T_{cr,pstc}$	Cracking strength of the torsional member in PT flat plate structures
A_s	Nonprestressed steel	T_g	Torsional moment induced by gravity loads
C	Torsional constant	T_l	Torsional moment induced by lateral loads
c_1	Column width in the loading direction	T_{tot}	Total moment in the torsional member due to gravity and lateral loads
c_2	Column width perpendicular to the design direction	V_c	Punching shear strength of the flat plate slab
E_c	Elastic modulus of concrete	V_g	Gravity shear force
f_1	Principal tensile stress	V_p	Vertical component of effective prestressing forces
f_c'	Compressive strength of concrete	λ_c	Load ratio factor
f_{cr}	Cracking strength of concrete	v	Shear stress on the web
f_{pc}	Compressive stress due to the prestress	v_{cr}	Shear cracking strength
K_c	Flexural stiffness of the column	θ_c	Rotation angle of the column
K_{ec}	Stiffness of an equivalent column	$\theta_{t,gravity}$	Rotational angle developed in the torsional member contributes to the rotation of the equivalent column
K_{es}	Stiffness of the equivalent slab	$\theta_{t,lateral}$	Rotation angle of the torsional member can be considered as contributing to the rotation of the equivalent slab
K_l	Actual flexural stiffness of the flat plate slab	θ_{total}	Rotation angle of the torsional member in the flat plate system subjected to gravity and lateral loads
K_o	Elastic flexural stiffness calculated using the gross section of the slab without a consideration of gravity loads	η_g	Stiffness reduction factor of the slab
K_s	Flexural stiffness of the slab	$\eta_{l,ext}$	Stiffness reduction factors of the torsional members for the exterior connections
$K_{s,eff}$	Effective flexural stiffness of the slab-beam member	$\eta_{l,int}$	Stiffness reduction factors of the torsional members for the interior connections
K_{tg}	Torsional stiffness of the torsional member in the RC flat plate slab system under gravity loads		
K_{tl}	Torsional stiffness of the torsional member in the flat plate system under lateral loads		
K_{t,λ_c}	Effective stiffness of a torsional member in the flat plate slab system subjected to gravity and lateral loads		
L_1	Span length width the design direction		
L_2	Span length width perpendicular to the design direction		
M_{ub}	Function of the unbalanced moment		
p_{cp}	Perimeter of the shear flow zone		